Oligomeric remodelling by molecular glues revealed using native mass spectrometry and mass photometry

Xiaojing Huang,[1] Hari Kamadurai,[2] Piro Siuti,[2] Ezaz Ahmed,[1,a] Jack L. Bennett,[1,b] and William A. Donald[1,*]

[1] School of Chemistry, University of New South Wales, Sydney, New South Wales 2052, Australia

[2] Triana Biomedicines Inc., Lexington, Massachusetts 02421, United States of America

* Corresponding author: w.donald@unsw.edu.au

Current addresses: a) Center for Synchrotron Biosciences, School of Medicine, Case Western Reserve University, Cleveland, Ohio 44106, United States of America; b) Department of Chemistry, University of Oxford, Oxford OX1 3QZ, United Kingdom

Abstract

Molecular glues stabilize interactions between E3 ligases and novel substrates to promote substrate degradation, thereby facilitating the inhibition of traditionally 'undruggable' protein targets. However, most known molecular glues have been discovered fortuitously or are based on well-established chemical scaffolds. Efficient approaches for discovering and characterising the effects of molecular glues on protein interactions are required to accelerate the discovery of novel agents. Here, we demonstrate that native mass spectrometry and mass photometry can provide unique insights into the physical mechanism of molecular glues, revealing previously unknown effects of such small molecules on the oligomeric organization of E3 ligases. When compared to well-established solution phase assays, native mass spectrometry provides accurate quantitative descriptions of molecular glue potency and efficacy while also enabling the binding specificity of E3 ligases to be determined in a single, rapid measurement. Such mechanistic insights should accelerate the rational development of molecular glues to afford powerful therapeutic agents.

Introduction

Small molecule drug discovery has been underpinned by the continual development of approaches to identify bioactive molecules that can modulate the activities of disease-involved proteins.[1] Although the traditional paradigm in medicinal chemistry is to target a specific protein of interest (POI) through direct interactions with a small molecule, approximately 80% of human proteins lack well-defined ligand-binding pockets and are classically considered 'undruggable'.[2,3] Such proteins can be destroyed by targeted protein degradation (TPD) via endogenous cellular mechanisms.[3] The two major approaches for TPD are hetero-bivalent proteolysis-targeted chimeras (PROTACs) and monovalent 'molecular glue' (MG) protein degraders which both promote proximity between an E3 ligase and POI resulting in protein degradation through the ubiquitin-proteasome system.[4] While the modular design of PROTACs, involving the connection of two 'warheads' via a linker, has been used to target over three hundred different proteins for degradation,[5] molecular glues are considerably less developed owing to analytical challenges in efficiently evaluating the activity of monovalent molecular glues for TPD and identifying inherently weak E3 ligase-target interactions that are potentially 'gluable'.[3] Thus, establishing rapid and efficient approaches for assessing molecular glues and discovering promising new E3-POI interactions is essential for the rational development of novel agents for TPD.

Two of the most well-established molecular glues that can promote highly cooperative interactions between an E3 ligase and a POI include the splicing inhibition sulphonamides (SPLAMs) and immunomodulatory imide drugs (IMiDs).[6] Both classes involve the cullin 4 (CUL4) E3 ligases, but contain different receptor subunits that interact with distinct substrates.[6] SPLAMs are a series of aryl sulphonamides, including E7820, indisulam, chloroquinoxaline sulfonamides (CQS), and tasisulam, that bind to the DDB1- and CUL4-associated factor 15 (DCAF15) subunit of $CUL4^{DCAF15}$. With the addition of a SPLAM, the splicing factor RNA-

binding motif protein 39 (RBM39) binds to the DCAF15-SPLAM complex (Figure 1a), leading to ubiquitination and subsequent proteasome-mediated degradation of the neosubstrate RBM39.[7,8] IMiDs include thalidomide and related derivatives (e.g. lenalidomide, pomalidomide) that interact with the cereblon subunit of the CUL4 E3 ligase ($CUL4^{CRBN}$) through the thalidomide binding domain, promote the formation of complexes with many different neosubstrates including the Ikaros zinc finger (IKZF) family proteins (Figure 1b).[3,9] Although neosubstrates such as G1 to S phase transition 1 (GSPT1) and casein kinase 1 alpha (CK1α) share minimal sequence homology with zinc finger proteins, they can also interact with $CUL4^{CRBN}$ through a conserved glycine-containing β-hairpin.[10,11] The degradation of GSPT1 without off-target degradation of zinc finger proteins has been demonstrated by using selective IMiDs such as CC-885.[10]

Currently, the potency and efficacy of molecular glues are primarily investigated by monitoring the ubiquitination and degradation of substrate proteins using cell-based assays, in addition to biophysical assays that explore interactions between glues and their targets.[10] A key physical criterion to assess the efficacy of a molecular glue is the extent to which MGs stabilize ternary complexes (E3-MG-neosubstrate), in addition to the binding affinity between the molecular glue and the E3 ligase. Isothermal titration calorimetry (ITC), surface plasmon resonance, and fluorophore-based techniques, such as fluorescence resonance energy transfer (FRET) have been used to investigate such interactions.[8,9,12] However, with optical and calorimetry-based approaches, the formation of ternary complexes can be challenging to directly deduce. The use of complementary approaches that can be used to directly confirm the formation of ternary complexes rapidly and sensitively with minimal sample consumption is desirable.

Native mass spectrometry and mass photometry are rapid, sensitive and label-free approaches that can be used to measure the stoichiometry of macromolecular assemblies.

Native mass spectrometry is particularly powerful for studying protein-ligand interactions,[13,14] while mass photometry enables protein-protein interactions to be measured at low nM concentrations[15,16] that are physiologically relevant for many E3 ligases.[17] A unique capability of native mass spectrometry compared to other solution-phase biophysical assays is that multiple non-covalent interactions can be screened rapidly and simultaneously. For example, native mass spectrometry can be used to screen thousands of small molecules for protein binding in one measurement,[18] and over ten protein-ligand dissociation constants can be obtained from a single mass spectrum.[19,20] However, native mass spectrometry and mass photometry are rarely used for characterising targeted protein degraders. Native mass spectrometry can be used to assess the efficacy of PROTACs (~1 kDa) in forming ternary E3-PROTAC-POI complexes (~55 kDa) and investigate substrate specificity.[21] In a very recent preprint,[22] native mass spectrometry was reported for identifying complexes formed between E3 ligases and proteins of interest upon binding with MGs at relatively high concentrations (100 μM MG to 5 μM E3 ligase). However, the extent that native mass spectrometry can be used to quantify the effectiveness of molecular glues in comparison to alternative solution-phase biochemical assays remains unclear. Moreover, the capacity for native mass spectrometry to identify weak E3 ligase-neosubstrate interactions in the absence of MGs, or explore substrate specificity has not been explored.

Here, we characterise the effects of molecular glues on the assembly of E3 ligases and protein targets using native mass spectrometry, mass photometry and an amplified luminescent proximity homogenous assay screen (AlphaScreen). Based on native mass spectrometry and mass photometry results, the well-characterised E3 ligase DCAF15[23] was found to associate into dimers and trimers at physiologically relevant concentrations (K_d values of ~7 and 9 nM for the dimer and trimer, respectively). Such higher order assemblies may have important impacts on drug efficacy. These oligomers can be disrupted by the investigational molecular

glues E7820, indisulam and tasisulam, forming monomeric DCAF15 complexes capable of associating with neosubstrates. These data suggest a secondary mechanism by which molecular glues regulate E3 ligase activity. Moreover, weak E3 ligase-protein interactions (~35 to 165 μM) in the absence of molecular glue can be readily measured by native mass spectrometry. Given that molecular glues typically act by enhancing inherently weak protein-protein interactions,[24] this approach should be useful in the future for identifying new ligase-POI interactions for the development of novel molecular glues. Quantitative measures of molecular glue potency derived from native mass spectrometry and AlphaScreen methods are in excellent agreement, and are consistent with previously reported data from ITC[25] and FRET[9,26] measurements. Moreover, native mass spectrometry can be employed to multiplex the quantitative measurement of such interactions, facilitating direct insights into the substrate specificity of key E3 ligases.

Results and discussion

Splicing inhibition sulphonamides (SPLAMs)

To explore the utility of native mass spectrometry in the characterisation of molecular glues, we first sought to study the formation of RBM39-DCAF15 complexes in the presence of several prototypical SPLAMs. Initially, to isolate the intact heterotrimeric DCAF15-DDB1-DDA1 E3 ligase, DCAF15 (Δ276-383, 6xHis-tagged), DDB1 (Δβ-propeller B) and DDA1 were co-expressed in *Spodoptera frugiperda* Sf9 insect cells and purified by successive rounds of immobilized metal affinity, anion exchange, and size-exclusion chromatography. When the resulting purified product was analysed by native mass spectrometry, five charge state distributions corresponding with distinct oligomeric assemblies could be resolved. Specifically, ions with masses in close agreement with the DDB1 monomer (18%), DDA1-DDB1 heterodimer (6%), and monomeric (6%), dimeric (45%), and trimeric (26%) DCAF15-DDB1-DDA1 assemblies (herein referred to as DCAF15) were detected (Figure 2a). Mass

photometry measurements of 20 nM DCAF15 in 100 mM ammonium acetate, pH 6.8 confirmed the presence of these assemblies in solution, with the most abundant peak centred at a mass of 95.8 ± 4.8 kDa corresponding with monomeric DDB1 (theoretical mass 93.1 kDa), and three additional lower abundance peaks with masses of 165.1 ± 8.3 kDa, 324.3 ± 16.2 kDa and 483.6 ± 24.2 kDa corresponding with monomeric (162.3 kDa), dimeric (324.6 kDa) and trimeric (486.9 kDa) DCAF15 (Figure 2d). The resolution of the mass photometry measurements[15] was not sufficient to resolve the binding of DDA1 (11.7 kDa) to DDB1 (93.1 kDa) explaining the apparent absence of this assembly from the mass distribution. Taken together, these results suggest that DDB1 is present in stoichiometric excess in solution, and are consistent with any dissociation of the intact DCAF15 being minimal during ion formation. Furthermore, it is indicated that DCAF15 can self-associate into dimeric and trimeric assemblies, providing a potential mechanism[27,28] for the regulation of ligase activity.

To assess whether the DCAF15 oligomers were formed at physiologically relevant concentrations, solutions containing 3.5 to 20 nM DCAF15 were analysed by mass photometry. Upon a decrease in concentration, the relative abundances of the DCAF15 monomer increased while that of the dimer and trimer decreased (Figure S1), with measured K_d values of ~7 nM and ~9 nM for the dimer and trimer, respectively (Table 1). These data indicate that the extent of DCAF15 oligomerisation is concentration dependent and mediated by non-covalent interactions at physiological relevant concentrations. Accordingly, an even greater extent of DCAF15 oligomerisation is observed for 5 μM of protein using native mass spectrometry (Figure 2a).

Following the generation and characterisation of the homotrimeric DCAF15 complex, we next sought to explore its interaction with RBM39 in the absence of molecular glues. When an equimolar quantity of RBM39 was added to the DCAF15 sample, an additional, highly abundant charge state distribution corresponding to monomeric RBM39 was observed by

native mass spectrometry (Figure 2b). The higher abundance of RBM39 ions compared to those for DCAF15 can be attributed to higher efficiencies for the formation and transfer of lower mass ions compared to higher mass ions under these conditions. Any peaks corresponding to RBM39 complexed with monomeric DCAF15 were at or slightly higher than the baseline noise level (Figures 2b). Increasing the ratio of RBM39:DCAF15 to 4:1 enabled the observation two additional charge state distributions corresponding with RBM39-DCAF15 and RBM39-$(DCAF15)_2$, consistent with a weak interaction between DCAF15 and RBM39 (Figure S2). Previously, weak interactions between DCAF15 and RBM39 (without molecular glue present) could not be readily detected using analytical ultracentrifugation,[29] which highlights the high sensitivity of native mass spectrometry for probing weak non-covalent interactions. These data suggest that native mass spectrometry may prove useful for detecting novel weak interactions between E3 ligases and neosubstrates that could be subsequently enhanced using rationally designed molecular glues.

Although DCAF15 was found to weakly interact with RBM39, it is unlikely that such a labile interaction would lead to significant complex formation and ubiquitination under physiological conditions. However, based on native mass spectrometry measurements, the apparent affinity of monomeric DCAF15 associating with one RBM39 increases significantly from K_d^{app} ~31-34 μM to K_d^{app} ~0.3-1.3 μM in the presence of 500 nM E7820 (Table 2). When 2.5 μM E7820 was added to a mixture of 5 μM RBM39 and 5 μM DCAF15, a relatively abundant DCAF15-E7820-RBM39 complex was observed in addition to a lower abundance RBM39-E7820-$(DCAF15)_2$ assembly (Figure 2c). Similar results were also observed at a lower molecular glue concentration (100 nM), in which RBM39 was found to interact with monomeric DCAF15 but any interaction with dimeric DCAF15 was undetectable (Figure 2d). Moreover, in both cases the oligomeric state of DCAF15 was found to shift substantially from trimer and dimer towards the monomer upon the addition of the molecular glue. For example,

the relative abundances of the trimer, dimer and monomer shifted from 34, 58 and 8% without MG present to 6, 73 and 21% with 2.5 μM E7820 added (Figure 2a, S3). Similar observations were also made using mass photometry, in which the addition of equimolar amounts of E2780 to DCAF15 (20 nM each) facilitated the dissociation of the DCAF15 trimer while dimers dissociation with both MGs and RBM39 added (Figure S4, Table 1). Such observations have not been clearly observed using other biophysical methods and suggest a secondary physical mechanism of action for molecular glues, in which E3 ligase activity is additionally regulated through 'oligomeric remodelling.' Upon such remodelling, the glue can subsequently stabilise interactions between monomeric DCAF15 and neosubstrates, initiating target ubiquitination.

In addition to E7820, three other aryl sulphonamide molecular glues (indisulam, CQS, and tasisulam) were also found to promote the formation of ternary complexes (K_d^{app} for 500 nM indisulam of ~0.4-1.4 μM, K_d^{app} for 500 nM CQS of ~0.5-1.7μM, and K_d^{app} for 500 nM of tasisulam of ~2.3-4.4 μM) (Table 2, Figure S5). To provide a measure of each drug's potency, we measured the extent of ternary complex formation as a function of glue concentration using native mass spectrometry (Figure 2f). Increasing the concentrations of glues was found to increase complex formation as expected. For example, at 100 nM of E7820, the relative abundance of the ternary complex RBM39-E7820-DCAF15 was ~22%, which increased to ~91% as the concentration of E7820 increased to 2.5 μM (Figure 2c-d,f). A similar concentration-dependent effect was observed for indisulam, CQS and tasisulam (Figure 2f) but differences in potency could be clearly observed. For example, 100 nM tasisulam has almost no effect in promoting complex formation (0.07 ± 0.01) while 100 nM E7820 had a significant effect (0.22 ± 0.03) (Figure 2f). To explore the utility of such quantitative measurements for drug characterisation, we compared the relative abundances of the corresponding ternary complex (RBM39-SPLAM-DCAF15) at 2.5 μM for each of the four active SPLAMs compared to the half maximal effective concentrations (EC50) obtained from an amplified luminescent

proximity homogeneous assay (AlphaScreen). The relative abundances of the ternary complexes from the native mass spectrometry experiments were inversely correlated with the EC50 values from AlphaScreen (Figure 2h). Thus, these data indicate that native mass spectrometry can be used to accurately assess the potency of molecular glues in promoting E3-neosubstrate interactions and should facilitate the development of novel approaches to quantify the effect of molecular glues on protein interactions in solution.

Immunomodulatory imide drugs (IMiDs)

To investigate the capacity for native mass spectrometry for elucidating ligase binding specificity in the presence of molecular glues, we examined the interactions of an additional CUL4 E3 ligase CRBN-DDB1 (hereafter CRBN), with three neosubstrates and three IMiDs using native mass spectrometry. These three neosubtrates were the second C2H2 zinc finger domain of Ikaros family zinc finger 1 ($IKZF1^{ZF2}$), Ikaros family zinc finger 2 ($IKZF2^{ZF2}$), and the C-terminal region (amino acids 300-496) of the G1 to S phase transition 1 (GSPT1) protein. Following expression and purification of the CRBN complex, native mass spectrometry and mass photometry revealed the presence of the intact complex, along with a stoichiometric excess of the DDB1 subunit (Figure S6a-b).

In the absence of IMiDs, the binary interaction between CRBN and the three neosubstrates was found to be weak but detectable. At a 1:1 ratio of $IKZF1^{ZF2}$:CRBN, ~13% of CRBN was observed to be in complex with $IKZF1^{ZF2}$ (Figure 3a) corresponding with an apparent K_d value of ~34 μM. Similarly, the K_d values for GSPT1 and $IKZF2^{ZF2}$ were measured to be ~163 μM and ~127 μM, respectively (Figure S7, Table 2). To date, neosubstrates are reported to recognised by CRBN only in the presence of IMiDs.[3] However, these data suggest that E3 ligases can weakly associate with neosubstrates in the absence of molecular glues, reinforcing the possibility that native mass spectrometry could be used to identify putative targets for molecular glue design.

Turning towards the interaction between the CRBN, IMiDs and neosubstrates, we first examined binding between the glue and CRBN in the absence of any substrate protein. Since the IMiD interact with CRBN though the thalidomide binding domain ($CRBN^{TBD}$), $CRBN^{TBD}$ was recombinantly expressed and purified from *Escherechia coli* for ligand binding assays using high-resolution native mass spectrometry. Although $CRBN^{TBD}$ interacts with the three IMiDs, the affinity is much lower than the full length CRBN-DDB1, consistent with previously reported results from ITC.[30] Specifically, the K_d values for the interaction of pomalidomide, lenalidomide and thalidomide with $CRBN^{TBD}$ were 14.7 ± 1.9, 6.7 ± 0.9, and 43.4 ± 2.6 μM, respectively (Figure S8) compared to less than 0.15 to 0.25 μM for these IMiDs with the CRBN-DDB1 based on previously reported ITC results.[25] Recently, the Lon-like domain (LLD) of CRBN was discovered to move into proximity with the thalidomide binding domain (TBD) upon IMiD binding, and this allosteric rearrangement is regulated by the DDB1 subunit.[31] The closed conformation of CRBN promotes stable association with neosubstrate.[31] These data presented here are also consistent with the LLD of CRBN and DDB1 augmenting the interaction of the TBD and IMiDs.[30] Moreover, it was also observed that $CRBN^{TBD}$ alone is not sufficient to recruit the neosubstrates $IKZF1^{ZF2}$, $IKZF2^{ZF2}$ or GSPT1 at up to 50 μM IMiDs, consistent with both domains of CRBN (i.e. TBD and LLD) and DDB1 being required for stable interactions with neosubstrates (Figure S9).

The CRBN complex with IMiDs and neosubstrates form stable ternary complexes based on results from native mass spectrometry. For example, the addition of 10 μM pomalidomide to 5 μM CRBN and 5 μM of either $IKZF1^{ZF2}$, GSPT1, or $IKZF2^{ZF2}$ resulted in the formation of ternary complexes for each neosubstrate with the lowest apparent K_d for CRBN and $IKZF1^{ZF2}$ at 3.4 ± 0.7 μM ($K_d{}^{app}{}_{IKZF1,pom}$), compared to the other two neosubstrates ($K_d{}^{app}{}_{GSPT1,pom}$ 7.3 ± 0.5 μM and $K_d{}^{app}{}_{IKZF2,pom}$ 15.9 ± 3.6 μM; Figure 3b-d, Table 2). That is, pomalidomide preferentially induces a preferential interaction between CRBN with $IKZF1^{ZF2}$

compared to the other neosubstrates, which is consistent with previous reports based on data from time-resolved FRET experiments.[9,26] Both zinc finger neosubtrates have the same sequence, except for a Q147H mutation in IKZF2^{ZF2}. This mutation results in a decrease in the binding affinity to pomalidomide-bound CRBN by 2-3 times based on *in vitro* time-resolved FRET experiments.[9] Thus, the general trend in the potency of pomalidomide for the three neosubstrates in terms of the apparent dissociation constants and extent of ternary complex formation that were obtained by native mass spectrometry is consistent with results from FRET-based experiments.

Other weak interactions could also be observed in the mixture upon the addition of neosubstrates with or without glue. Specifically, IKZF1^{ZF2}-DDB1 and IKZF2^{ZF}-DDB1 complexes were detected with comparable abundances with or without the addition of IMiDs using native mass spectrometry (Figure 3a-d). However, no interactions between GSTP1 and free DDB1 were observed (Figure S10). These results are consistent with previous reports that DDB1 can interact with the zinc finger domain of viral proteins based on pull-down assays and X-ray crystallography.[32–34]

For CRBN, the extent of ternary complex formation for the three neosubstrates was measured by native mass spectrometry as a function of IMiD (pomalidamide, lenalidomide, and thalidomide) concentration. For eight of nine potential ternary complexes, the extent of ternary complex formation increased as the concentration of the molecular glue increased from 2.5 to 10 μM (Figure 3e-g) except for the combination of the least potent IMiD thalidomide with the lowest affinity neosubstrate IKZF2^{ZF2}. In Figure 3h, the extent of ternary complex formation for CRBN with IKZF1^{ZF2}, IKZF2^{ZF2} and GSTP1 for all three IMiDs at 10 μM are compared to the K_d values for CRBN-IMiD that were reported previously based on isothermal titration calorimetry (ITC) measurements.[25] For all three neosubstrates, the use of pomalidomide resulted in the greatest extent of ternary complex formation using native mass

spectrometry, which correlates with pomalidomide having the highest binding affinity (K_d of 0.157 μM) of the three IMiDs.

To explore the potential of using native mass spectrometry to reveal the binding specificity of an E3 ligase for neosubstrates in a pooled mixture of proteins, CRBN was incubated with equimolar IKZF1^{ZF2}, IKZF1^{ZF2}, and GSPT1. Without the addition of an IMiD, native mass spectrometry resulted in the formation of ions corresponding to all three potential CRBN-neosubstrate complexes (Figure S11). The addition of pomalidomide at 50 μM into the pooled mixture of CRBN with all three neosubstrates resulted in the formation of IKZF1^{ZF2}-CRBN-pomalidomide in significantly higher abundance than CRBN complexed with the other neosubstrates (Figure 4a). A minor amount of DDB1 was also complexed to IKZF1^{ZF2} or IKZF2^{ZF2} under these conditions (Figure 4a, S12). All ternary complexes and unbound CRBN were detectable using native mass spectrometry, and the order of neosubstrate specificity agreed with the individual experiments in which neosubstrates were not pooled. In the multiplexing experiments, lenalidomide and thalidomide also induce ternary complex formation with a strong preference for CRBN-IMiDs binding to IKZF1^{ZF2} rather than GSPT1 and IKZF2^{ZF2} (Figure 4b, S12). DCAF15 recruitment of RBM39 can also be readily measured by native mass spectrometry in a mixture of five additional proteins (ubiquitin, cytochrome *c*, lysozyme, β-lactoglobulin monomer and dimer, and bovine serum albumin) at a concentration of 50 μM E7820 (Figure S13). These results indicate that native mass spectrometry can be used to efficiently examine neosubstrate specificity using rapid and sensitive multiplexed measurements.

Conclusions

The efficacy of molecular glues in stabilizing E3 ligase-neosubstrate interactions can be efficiently assessed using native mass spectrometry, as demonstrated for two E3 ligases (CRBN and DCAF15), four targets (IKZF1^{ZF2}, IKZF2^{ZF2}, GSPT1, and RBM39), and seven

MGs. The extent of ternary complex formation obtained using native mass spectrometry correlates with data from well-established FRET, AlphaScreen and ITC experiments. In addition, the native mass spectrometry results agree well with data from solution-phase mass photometry experiments. For example, based on mass photometry, DCAF15 self assembles into dimers (K_d of 7 ± 3 nM) and trimers (9 ± 4 nM) at low, physiologically relevant concentrations and the stoichiometric addition of a molecular glue significantly lowers the binding affinity of the oligomeric complexes (K_d values of 16 ± 1 and 26 ± 4 nM for dimer and trimer respectively) to favour the formation of monomeric DCAF15, consistent with results from native mass spectrometry experiments.

When compared to alternate approaches for elucidating molecular glue function, native mass spectrometry provides unique insights into the remodelling of oligomeric states by the molecular glues. Specifically, this study enabled the detection of weak ligase-neosubstrate interactions in the absence of glues that have not been observed using more traditional approaches. Dimers and trimers of DCAF15 can be disassembled by molecular glues, suggesting a potential secondary mechanism by which glues can regulate E3 ligase activity. Moreover, the binding specificity of a ligase for multiple targets could be measured simultaneously using pooled mixtures of multiple potential proteins-of-interest in a single native mass spectrometry measurement. By providing detailed mechanistic insights, native mass spectrometry should be beneficial in accelerating the discovery new molecular glues and E3 ligase-target pairs to advance the development of novel therapeutic treatments.

Material and methods

Protein expression and purification

Full details of the expression and purification of DCAF15-DDB1-DDA1, RBM39, CRBN-DDB1, $CRBN^{TBD}$, $IKZF1^{ZF2}$, $IKZF2^{ZF2}$, and GSPT1 are found in the Supporting Information.

Native mass spectrometry

All molecular glues were dissolved in DMSO at 10 mM or 20 mM. A series of dilutions were used to ensure the concentration of DMSO remained at 0.5% in all solutions that were analyzed by native mass spectrometry unless specified otherwise. All recombinant proteins were buffer exchanged into 100 mM ammonium acetate (pH 6.8) using self-packed gel filtration columns (Bio-Gel P-6 polyacrylamide beads in 1.1 ml spin columns, BioRad). Proteins were passed through the gel filtration columns twice before their concentrations were measured using a microvolume spectrophotometer (NanoDrop 1000, Thermo Fisher Scientific).

Nanoscale ion emitters with an inner bore diameter of ~680 nm at the tip were fabricated from borosilicate glass capillaries using a Flaming/Brown type microcapillary puller (P-97, Sutter Instrument Company) as previously described.[20] To enable charge transfer between the instrument source and analyte solution, the ion emitters were sputter coated with a mixture of gold and palladium (1.5 kV, 20 mA, 0.1 mbar; Scancoat 6, Edwards). Native mass spectrometry measurements were acquired using a hybrid quadrupole−time-of-flight mass spectrometer (Ultima, Waters) equipped with an nanoelectrospray ionization (nESI) source. Solutions containing 5 μM of each protein in 100 mM NH_4OAc (pH 6.8) were used throughout unless specified otherwise. The nESI voltage applied to the emitter tip relative to the heated capillary inlet (60˚C) was +0.8 to 1.5 kV. The cone voltage offset and RF lens 1 voltage offset were set to 100 V each. All mass spectra were acquired with a scan time of 1.0 sec and an interscan time of 0.1 sec in triplicate.

Mass spectra were processed and smoothed using Masslynx V4.2. The abundances of the ternary complexes were obtained from the peak areas in the deconvoluted spectra using UniDec 5.2.1.[35] The relative abundances were plotted as the fraction of the complex to all ions containing the specific E3 of interest using GraphPad Prism 9.3.1. Spectra were annotated using NaViA 1.0.[36]

Affinity measurements

To quantify protein-ligand dissociation constants for IMiD-CRBN interaction, triplicate measurements of 10 μM $CRBN^{TBD}$ incubated with 7.5 μM to 15 μM of ImiDs were acquired using a hybrid ion trap-Orbitrap mass spectrometer (LTQ Orbitrap XL, Thermo Fisher Scientific). The peak areas for the 6+ and 7+ charge states were used to quantify protein-ligand dissociation constants as previously described.[20]

The apparent protein-protein dissociation constants for the neosubstrate-E3 complexes with or without molecular glue were calculated from 5 μM E3 ligase and 5 μM neosubstrate using a hybrid quadrupole-time-of-flight mass spectrometer. By assuming that the neosubstrate-E3 complexes have a comparable response factor to E3 alone (CRBN or monomeric DCAF15), K_d^{app} values could be calculated from triplicate deconvoluted spectra as previously reported for protein-ligand interactions.[20] Due to the stoichiometric excess of DDB1 subunit and self-oligomerization in the E3 ligase samples, the effective concentrations of monomeric DCAF15 and CRBN were lower than the calculated from absorbance at 280 nm (A_{280}). To correct for the E3 concentration, a weighted average of extinction coefficient of all species based on the ratio in native mass spectrometry was used to convert A_{280} into concentrations. Since different ions inevitably have different ionization efficiency in native mass spectrometry, a true E3 concentration would lie between 5 μM and the corrected concentrations.

Mass photometry

Solution-phase, interferometric scattering mass spectrometry measurements were acquired using a commercial mass photometer (TwoMP, Refeyn). A solvent blank of 15 μl of 100 mM ammonium acetate was acquired immediately prior to adding solutions containing proteins. A mass calibration was performed for each sample carrier slide by adding a 5 μl of NativeMark™ Unstained standard (Thermo Fisher Scientific) diluted 75 times in 100 mM

aqueous ammonium acetate into a 15 µl of a droplet of 100 mM aqueous ammonium acetate. The resulting peaks in the mass photometry spectrum corresponding to bovine serum albumin (66 kDa), lactate dehydrogenase (146 kDa), apo-ferritin (480 kDa), and IgM pentamer (1048 kDa) were fitted with Gaussian functions to obtain their centroids, which were used to linearly calibrate all reported spectra for that specific slide. A two µl droplet of each protein sample was applied onto a 15 µl droplet to a final concentration of 20 nM or less in 100 mM aqueous ammonium acetate. A mass photometry video of both the calibration and the sample solutions were recorded for 1 min and analysed by DiscoverMP 2.3.0 (Refeyn). The apparent dimeric and trimeric DCAF15 dissociation constants ($K_{d,dimer}$ and $K_{d,trimer}$) were calculated by [monomer]^2/[dimer] and [trimer]/[dimer]x[monomer] respectively.

Amplified luminescent proximity homogeneous assay

MG-induced ternary complex formation was monitored using amplified luminescent proximity homogeneous assays (AlphaLISA®, Perkin Elmer). Test compounds were first collected in a 384-well microplate (Grenier Bio-One, 781280) as 2 mM stocks in DMSO. These stocks were then serially diluted in DMSO by 3-fold into a new plate using a liquid handling robot (mosquito® HTS, SPT Labtech). In duplicate wells, 0.2 ul of the diluted stocks were then dispensed into a 384-well Optiplate (Perkin Elmer, 6007290). Separately, a protein mixture consisting of His-tagged DCAF15 complex and biotin-carrying RBM39 (204 nM each) was prepared in reaction buffer (50 mM HEPES, pH 7.5, 100 mM NaCl, 2 mM MgCl2, 1 mg/ml BSA, 2 mM TCEP, 0.05% Tween-20). A 9.8 µl aliquot of the protein mixture was then mixed with the compounds in the assay plate and incubated for one hour at room temperature. Reaction mixtures with no compounds added were included as negative controls, while a His-tagged and biotinylated GST protein was included to track general assay performance. Nickel chelate AlphaLISA acceptor beads (Perkin Elmer, AL108M) and AlphaScreen streptavidin donor beads (Perkin Elmer, 6760002) were prepared separately in the reaction buffer at 80

μg/ml. The beads were then added to the assay plate sequentially to a final concentration of 20 μg/ml with incubation at room temperature for 1-2 hours after each addition. Signals were recorded using a plate reader (EnVision 2104 Multilabel Plate Reader, Perkin Elmer) with excitation wavelength of 680 nm and emission wavelength of 615 nm. The dose response curves were generated in GraphPad Prism 7.0 to obtain the half maximal effective concentration (EC50).

Conflict of interest disclosure

This research was supported by Triana Biomedicines Inc., a venture-backed biopharmaceutical company.

Acknowledgements

W.A.D. acknowledges financial support from Australian Research Council (FT200100798). We thank the Structural Biology and the Bioanalytical Mass Spectrometry facilities of the Mark Wainwright Analytical Center (UNSW Sydney) for access to instrumentation.

Figures and figure captions

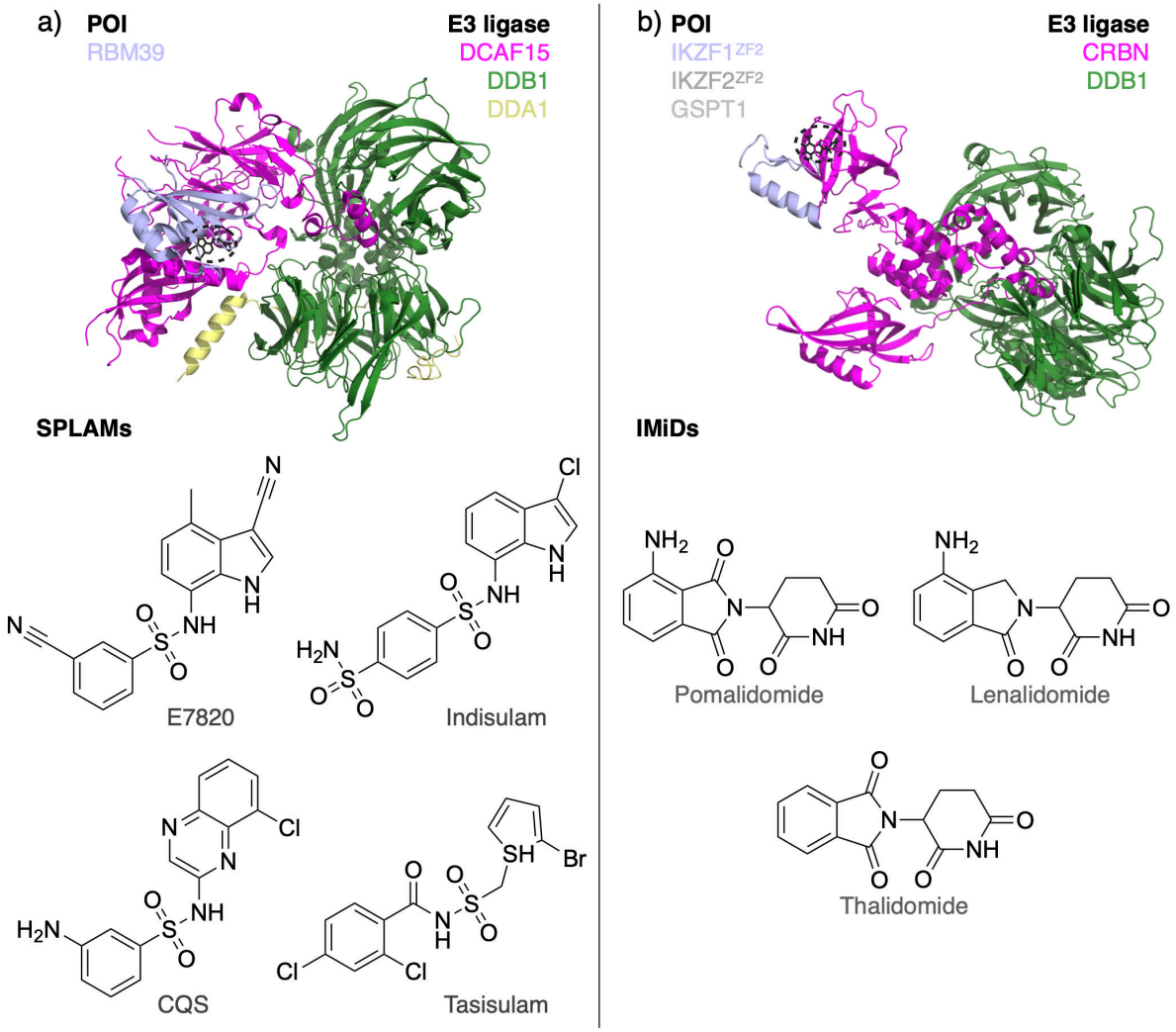

Figure 1. Molecular glues stabilize interactions between E3 ligases and therapeutically relevant substrates to initiate substrate degradation. a) Structure of the DCAF15-DDB1-DDA1:RBM39 complex formed in the presence of the molecular glue (MG) E7820 (PDB 6Q0R).[8] b) Structure of the CRBN-DDB1:IKZF1^{ZF2} complex stabilized by pomalidomide (PDB 6H0F).[9] Alternate neosubstrates and the structures of molecular glues investigated herein are also listed.

Table 1. Apparent K_d values for the DCAF15 homodimer and homotrimer obtained from mass photometry measurements.

DCAF15 (20 nM)	RBM39 (20 nM)	E7820	$K_{d,dimer}$ (nM)[a]		$K_{d,trimer}$ (nM)[a]	
			Mean	*SD*	*Mean*	*SD*
+	-	-	7	3	9	4
+	-	20 nM	16	1	26	4
+	+	-	10	4	10	6
+	+	20 nM	21	4	21	2
+	+	200 nM	23	3	23	2

[a] The mean and standard deviation (SD) of the apparent dissociation constants was obtained for dimer dissociating into monomer and trimer dissociating into dimer and monomer from three replicates from the relative abundances of DCAF15 monomers and oligomers (refer to Figure S4).

Table 2. Estimated apparent K_d values for neosubstrate-E3 ligase interactions obtained with or without a correction[a] for the concentration of DCAF and CRBN in solution.

DCAF15	RBM39	SPLAMs (500 nM)	DCAF15 uncorrected 5 μM		DCAF15 corrected 2.06 μM[a]	
			Mean	*SD*	*Mean*	*SD*
+	+	-	31	15	34	20
+	+	E7820	0.3	0.1	1.3	0.3
+	+	indisulam	0.4	0.6	1.4	1.2
+	+	CQS	0.5	0.2	1.7	0.3
+	+	tasisulam	2.3	2.4	4.4	3.1
CRBN	Target	Pomalidomide (10 μM)	CRBN uncorrected 5 μM		CRBN corrected 4.36 μM[a]	
			Mean	*SD*	*Mean*	*SD*
+	$IKZF1^{ZF2}$	-	35	2	34	2
+	$IKZF1^{ZF2}$	+	3.4	0.7	3.8	0.7
+	$IKZF2^{ZF2}$	-	128	21	127	22
+	$IKZF2^{ZF2}$	+	15.9	3.6	16.4	3.6
+	GSPT1	-	164	34	163	35
+	GSPT1	+	7.3	0.5	7.8	0.5

[a] The measured initial concentration of DCAF and CRBN in solution are lower than that calculated using ultraviolet absorbance at 280 nm owing to a stoichiometric excess of DDB1, and the self-oligomerization of DCAF15. To correct for these factors, the concentrations of DCAF and CRBN can be approximated by assuming the ionization efficiencies of all species are the same in native mass spectrometry. However, this likely underestimates the concentration of these complexes. Thus, the actual K_d values are somewhere between the uncorrected and corrected values.

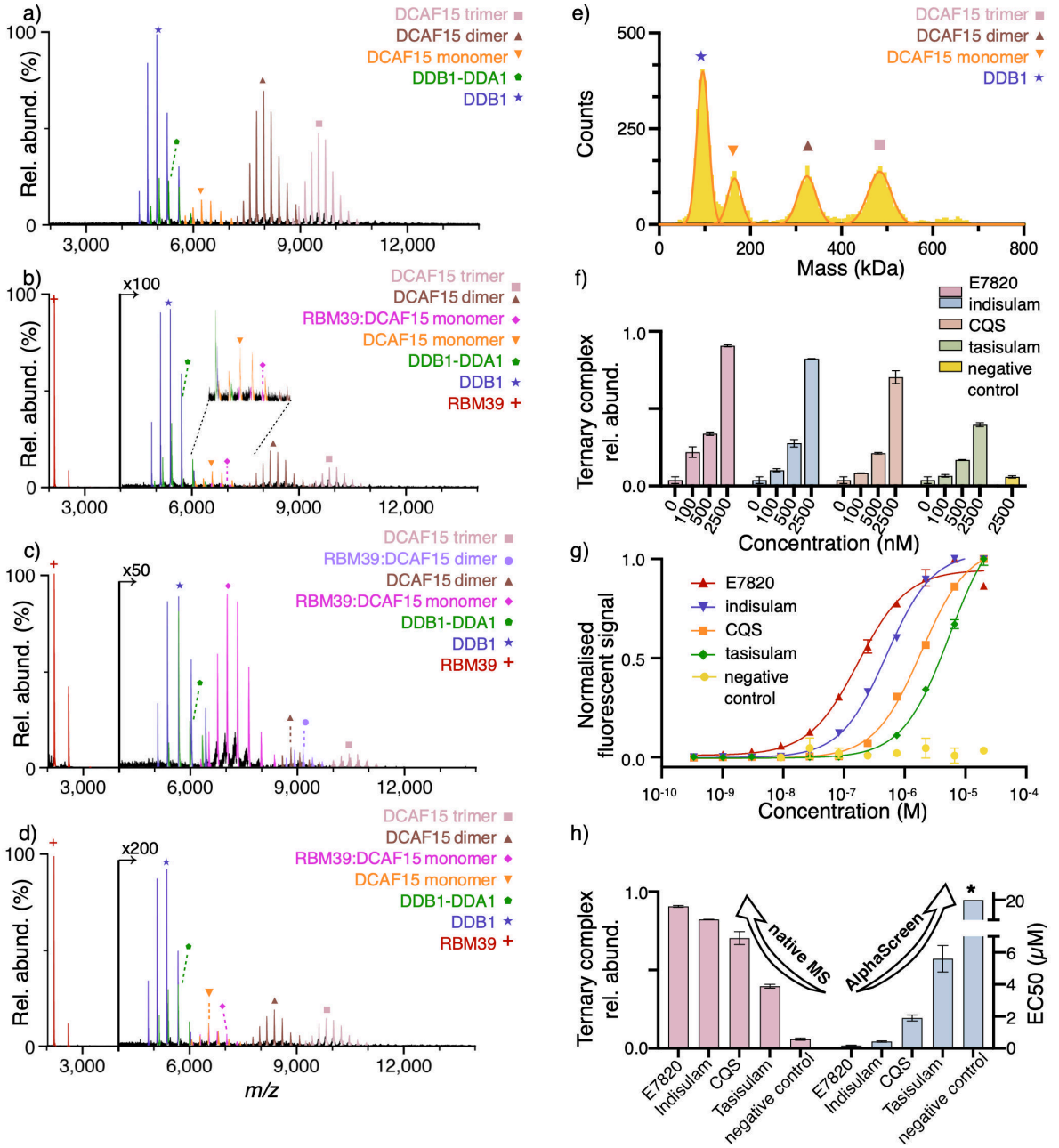

Figure 2. Native mass spectrometry can be used to assess the efficacy of SPLAMs in promoting interactions between DCAF15-DDB1-DDA1 (DCAF15) and the neosubstrate, RBM39. Native mass spectra of a) 5 μM of DCAF15, b) 5:5 μM RBM39:DCAF15, and 5:5 μM RBM39:DCAF15 and c) 2.5 μM E7820 or d) 0.1 μM E7820 in 100 mM NH_4OAc (pH 6.8) and 0.5% DMSO. e) Mass photometry mass distribution (N ≥ 3 replicates) of 20 nM DCAF15 in 100 mM NH_4OAc. f) Plot of the concentration dependent effect of SPLAMs on ternary complex formation as measured by native mass spectrometry. Relative abundances are defined as the abundance of the ternary complex as a proportion of all DCAF15-containing species. Even at 2.5 μM, an aryl sulphonamide negative control (N-[4-(quinoxalin-2-ylsulfamoyl)phenyl]acetamide) did not induce significant complex formation. g) Amplified luminescent proximity homogeneous assay (AlphaScreen) dose response curves obtained for different concentrations of SPLAMs with a 1:1 mixture of RBM39:DCAF15 (200 nM each; N = 2). h) Plot of the abundances of ternary complexes for 2.5 μM of each SPLAM observed by native mass spectrometry, and the half maximal effective concentrations (EC50) of SPLAMs from AlphaScreen. Asterisk indicates an EC50 value that is greater than 20 μM.

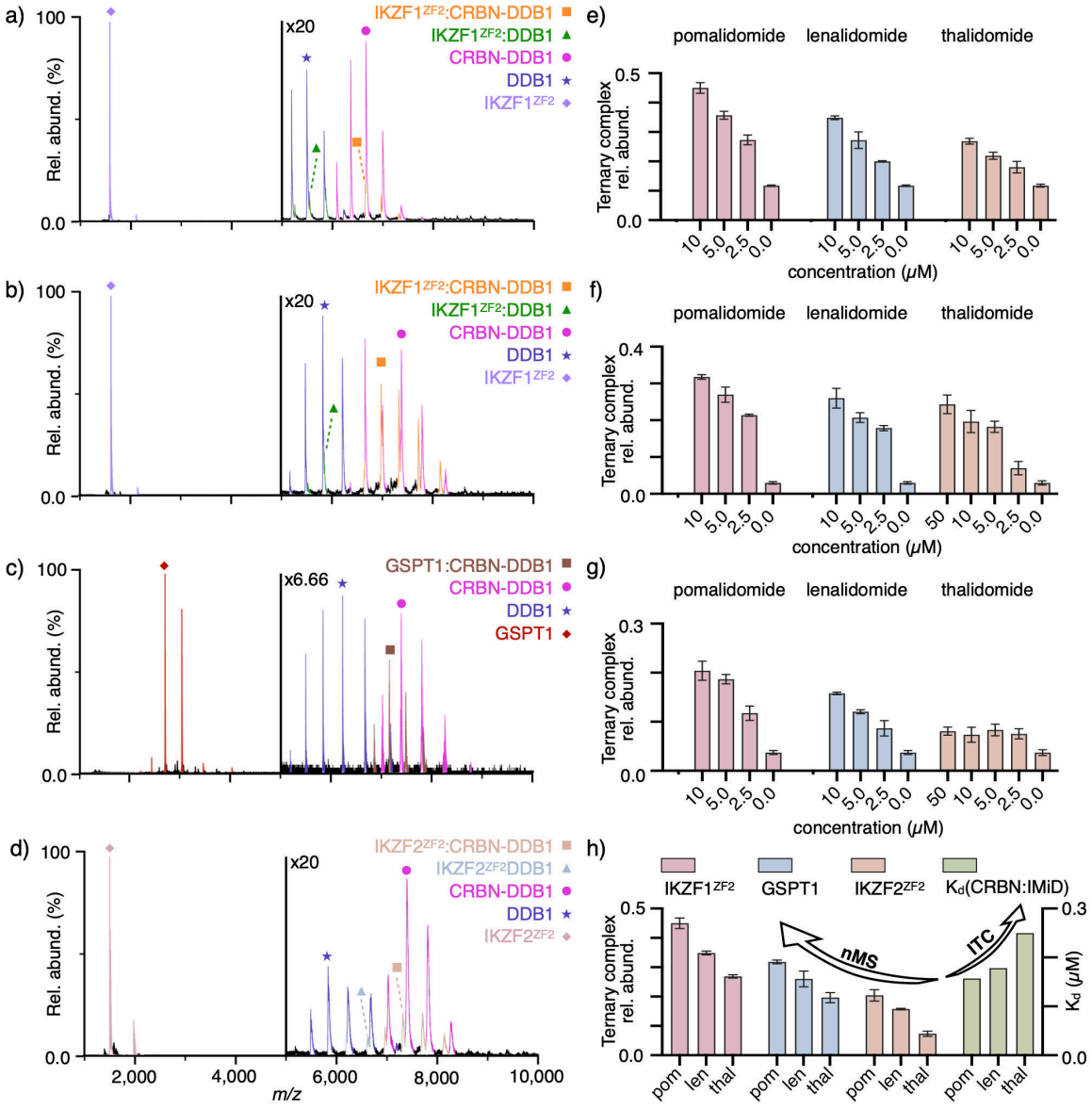

Figure 3. Differential potency of immunomodulatory imide drugs (IMiDs) in enhancing interactions between CRBN-DDB1 (CRBN) and its neosubstrates. a) Native mass spectrum of 5 µM of IKZF1^{ZF2} and 5 µM CRBN in 100 mM NH_4OAc (pH 6.8) and 0.5% DMSO. Even in the absence of a molecular glue, the IKZF1^{ZF2}-CRBN complex can be observed in low abundance. b-d) Native mass spectra of CRBN and b) IKZF1^{ZF2}, c) GSPT1, or d) IKZF2^{ZF2} (5 µM each) with 10 µM pomalidomide in 100 mM NH_4OAc (pH 6.8) and 0.5% DMSO. Addition of the glue promotes interactions between CRBN and each neosubstrate. e-g) Plots of the concentration dependent effect of pomalidomide (pom), lenalidomide (len), and thalidomide (thal) on the relative abundance of the complex formed between CRBN, the IMiD and e) IKZF1^{ZF2}, f) GSPT1, and g) IKZF2^{ZF2}. Relative abundances are defined as the abundance of the ternary complex as a proportion of all CRBN-containing species. Error bars correspond to the standard deviation from three replicates. h) Comparison between the ternary complex abundances at 10 µM for each IMiD and previously reported K_d values[25] for CRBN and each IMiD as measured by ITC.

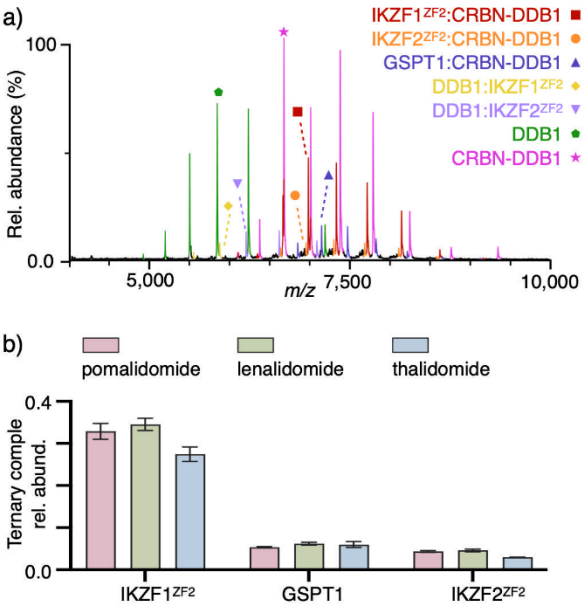

Figure 4. Multiplexed screening of neosubstrate interactions with CRBN using native mass spectrometry. a) Native mass spectrum of CRBN, IKZF1^{ZF2}, IKZF2^{ZF2}, and GSPT1 (5 µM each) with 50 µM pomalidomide in 100 mM NH_4OAc (pH 6.8) and 0.5% DMSO. b) Relative abundance of the CRBN-IMiD-neosubstrate complexes within the mixture of CRBN and three neosubstrates (5 µM each) in the presence of 50 µM pomalidomide, lenalidomide, or thalidomide. Error bars correspond to the standard deviation of triplicate measurements.

Table of contents graphic

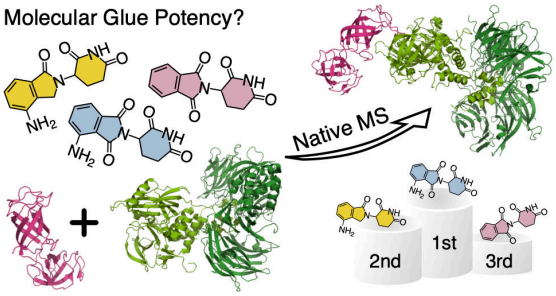

References

(1) Bedard, P. L.; Hyman, D. M.; Davids, M. S.; Siu, L. L. Small Molecules, Big Impact: 20 Years of Targeted Therapy in Oncology. *The Lancet* **2020**, *395* (10229), 1078–1088.

(2) Henley, M. J.; Koehler, A. N. Advances in Targeting 'Undruggable' Transcription Factors with Small Molecules. *Nat Rev Drug Discov* **2021**, *20* (9), 669–688.

(3) Yamamoto, J.; Ito, T.; Yamaguchi, Y.; Handa, H. Discovery of CRBN as a Target of Thalidomide: A Breakthrough for Progress in the Development of Protein Degraders. *Chemical Society Reviews* **2022**, *51* (15), 6234–6250.

(4) Li, X.; Song, Y. Proteolysis-Targeting Chimera (PROTAC) for Targeted Protein Degradation and Cancer Therapy. *Journal of Hematology & Oncology* **2020**, *13* (1), 50.

(5) Weng, G.; Cai, X.; Cao, D.; Du, H.; Shen, C.; Deng, Y.; He, Q.; Yang, B.; Li, D.; Hou, T. PROTAC-DB 2.0: An Updated Database of PROTACs. *Nucleic Acids Research* **2023**, *51* (D1), D1367–D1372.

(6) Domostegui, A.; Nieto-Barrado, L.; Perez-Lopez, C.; Mayor-Ruiz, C. Chasing Molecular Glue Degraders: Screening Approaches. *Chemical Society Reviews* **2022**, *51* (13), 5498–5517.

(7) Xu, Y.; Nijhuis, A.; Keun, H. C. RNA-Binding Motif Protein 39 (RBM39): An Emerging Cancer Target. *British Journal of Pharmacology* **2022**, *179* (12), 2795–2812.

(8) Faust, T. B.; Yoon, H.; Nowak, R. P.; Donovan, K. A.; Li, Z.; Cai, Q.; Eleuteri, N. A.; Zhang, T.; Gray, N. S.; Fischer, E. S. Structural Complementarity Facilitates E7820-Mediated Degradation of RBM39 by DCAF15. *Nat Chem Biol* **2020**, *16* (1), 7–14.

(9) Sievers, Q. L.; Petzold, G.; Bunker, R. D.; Renneville, A.; Słabicki, M.; Liddicoat, B. J.; Abdulrahman, W.; Mikkelsen, T.; Ebert, B. L.; Thomä, N. H. Defining the Human C2H2 Zinc-Finger Degrome Targeted by Thalidomide Analogs through CRBN. *Science* **2018**, *362* (6414), eaat0572.

(10) Matyskiela, M. E.; Lu, G.; Ito, T.; Pagarigan, B.; Lu, C.-C.; Miller, K.; Fang, W.; Wang, N.-Y.; Nguyen, D.; Houston, J.; Carmel, G.; Tran, T.; Riley, M.; Nosaka, L.; Lander, G. C.; Gaidarova, S.; Xu, S.; Ruchelman, A. L.; Handa, H.; Carmichael, J.; Daniel, T. O.; Cathers, B. E.; Lopez-Girona, A.; Chamberlain, P. P. A Novel Cereblon Modulator Recruits GSPT1 to the CRL4CRBN Ubiquitin Ligase. *Nature* **2016**, *535* (7611), 252–257.

(11) Petzold, G.; Fischer, E. S.; Thomä, N. H. Structural Basis of Lenalidomide-Induced CK1α Degradation by the CRL4CRBN Ubiquitin Ligase. *Nature* **2016**, *532* (7597), 127–130.

(12) Milroy, L.-G.; Grossmann, T. N.; Hennig, S.; Brunsveld, L.; Ottmann, C. Modulators of Protein–Protein Interactions. *Chem. Rev.* **2014**, *114* (9), 4695–4748.

(13) Tamara, S.; den Boer, M. A.; Heck, A. J. R. High-Resolution Native Mass Spectrometry. *Chem. Rev.* **2022**, *122* (8), 7269–7326. https://doi.org/10.1021/acs.chemrev.1c00212.

(14) Bennett, J. L.; Nguyen, G. T. H.; Donald, W. A. Protein–Small Molecule Interactions in Native Mass Spectrometry. *Chem. Rev.* **2022**, *122* (8), 7327–7385.

(15) Young, G.; Hundt, N.; Cole, D.; Fineberg, A.; Andrecka, J.; Tyler, A.; Olerinyova, A.; Ansari, A.; Marklund, E. G.; Collier, M. P.; Chandler, S. A.; Tkachenko, O.; Allen, J.; Crispin, M.; Billington, N.; Takagi, Y.; Sellers, J. R.; Eichmann, C.; Selenko, P.; Frey, L.; Riek, R.; Galpin, M. R.; Struwe, W. B.; Benesch, J. L. P.; Kukura, P. Quantitative Mass Imaging of Single Biological Macromolecules. *Science* **2018**, *360* (6387), 423–427.

(16) Soltermann, F.; Foley, E. D. B.; Pagnoni, V.; Galpin, M.; Benesch, J. L. P.; Kukura, P.; Struwe, W. B. Quantifying Protein–Protein Interactions by Molecular Counting with

Mass Photometry. *Angewandte Chemie International Edition* **2020**, *59* (27), 10774–10779.
(17) Reichermeier, K. M.; Straube, R.; Reitsma, J. M.; Sweredoski, M. J.; Rose, C. M.; Moradian, A.; Besten, W. den; Hinkle, T.; Verschueren, E.; Petzold, G.; Thomä, N. H.; Wertz, I. E.; Deshaies, R. J.; Kirkpatrick, D. S. PIKES Analysis Reveals Response to Degraders and Key Regulatory Mechanisms of the CRL4 Network. *Molecular Cell* **2020**, *77* (5), 1092-1106.e9.
(18) Nguyen, G. T. H.; Bennett, J. L.; Liu, S.; Hancock, S. E.; Winter, D. L.; Glover, D. J.; Donald, W. A. Multiplexed Screening of Thousands of Natural Products for Protein–Ligand Binding in Native Mass Spectrometry. *J. Am. Chem. Soc.* **2021**, *143* (50), 21379–21387.
(19) Nguyen, G. T. H.; Nocentini, A.; Angeli, A.; Gratteri, P.; Supuran, C. T.; Donald, W. A. Perfluoroalkyl Substances of Significant Environmental Concern Can Strongly Inhibit Human Carbonic Anhydrase Isozymes. *Anal. Chem.* **2020**, *92* (6), 4614–4622.
(20) Nguyen, G. T. H.; Tran, T. N.; Podgorski, M. N.; Bell, S. G.; Supuran, C. T.; Donald, W. A. Nanoscale Ion Emitters in Native Mass Spectrometry for Measuring Ligand–Protein Binding Affinities. *ACS Cent. Sci.* **2019**, *5* (2), 308–318.
(21) Beveridge, R.; Kessler, D.; Rumpel, K.; Ettmayer, P.; Meinhart, A.; Clausen, T. Native Mass Spectrometry Can Effectively Predict PROTAC Efficacy. *ACS Cent. Sci.* **2020**, *6* (7), 1223–1230.
(22) Jackson, C.; Beveridge, R. Native Mass Spectrometry of Complexes Formed by Molecular Glues Revealed Stoichiometric Rearrangement of the DCAF15 E3 Ligase. bioRxiv February 3, 2023, p 2023.02.03.526954.
(23) Han, T.; Goralski, M.; Gaskill, N.; Capota, E.; Kim, J.; Ting, T. C.; Xie, Y.; Williams, N. S.; Nijhawan, D. Anticancer Sulfonamides Target Splicing by Inducing RBM39 Degradation via Recruitment to DCAF15. *Science* **2017**, *356* (6336), eaal3755.
(24) Cao, S.; Kang, S.; Mao, H.; Yao, J.; Gu, L.; Zheng, N. Defining Molecular Glues with a Dual-Nanobody Cannabidiol Sensor. *Nat Commun* **2022**, *13* (1), 815.
(25) Fischer, E. S.; Böhm, K.; Lydeard, J. R.; Yang, H.; Stadler, M. B.; Cavadini, S.; Nagel, J.; Serluca, F.; Acker, V.; Lingaraju, G. M.; Tichkule, R. B.; Schebesta, M.; Forrester, W. C.; Schirle, M.; Hassiepen, U.; Ottl, J.; Hild, M.; Beckwith, R. E. J.; Harper, J. W.; Jenkins, J. L.; Thomä, N. H. Structure of the DDB1–CRBN E3 Ubiquitin Ligase in Complex with Thalidomide. *Nature* **2014**, *512* (7512), 49–53.
(26) Powell, C. E.; Du, G.; Che, J.; He, Z.; Donovan, K. A.; Yue, H.; Wang, E. S.; Nowak, R. P.; Zhang, T.; Fischer, E. S.; Gray, N. S. Selective Degradation of GSPT1 by Cereblon Modulators Identified via a Focused Combinatorial Library. *ACS Chem Biol* **2020**, *15* (10), 2722–2730.
(27) Marianayagam, N. J.; Sunde, M.; Matthews, J. M. The Power of Two: Protein Dimerization in Biology. *Trends in Biochemical Sciences* **2004**, *29* (11), 618–625.
(28) Gasper, R.; Meyer, S.; Gotthardt, K.; Sirajuddin, M.; Wittinghofer, A. It Takes Two to Tango: Regulation of G Proteins by Dimerization. *Nat Rev Mol Cell Biol* **2009**, *10* (6), 423–429.
(29) Bussiere, D. E.; Xie, L.; Srinivas, H.; Shu, W.; Burke, A.; Be, C.; Zhao, J.; Godbole, A.; King, D.; Karki, R. G.; Hornak, V.; Xu, F.; Cobb, J.; Carte, N.; Frank, A. O.; Frommlet, A.; Graff, P.; Knapp, M.; Fazal, A.; Okram, B.; Jiang, S.; Michellys, P.-Y.; Beckwith, R.; Voshol, H.; Wiesmann, C.; Solomon, J. M.; Paulk, J. Structural Basis of Indisulam-Mediated RBM39 Recruitment to DCAF15 E3 Ligase Complex. *Nat Chem Biol* **2020**, *16* (1), 15–23.
(30) Akuffo, A. A.; Alontaga, A. Y.; Metcalf, R.; Beatty, M. S.; Becker, A.; McDaniel, J. M.; Hesterberg, R. S.; Goodheart, W. E.; Gunawan, S.; Ayaz, M.; Yang, Y.; Karim, M. R.;

Orobello, M. E.; Daniel, K.; Guida, W.; Yoder, J. A.; Rajadhyaksha, A. M.; Schönbrunn, E.; Lawrence, H. R.; Lawrence, N. J.; Epling-Burnette, P. K. Ligand-Mediated Protein Degradation Reveals Functional Conservation among Sequence Variants of the CUL4-Type E3 Ligase Substrate Receptor Cereblon. *J Biol Chem* **2018**, *293* (16), 6187–6200.

(31) Watson, E. R.; Novick, S.; Matyskiela, M. E.; Chamberlain, P. P.; H. de la Peña, A.; Zhu, J.; Tran, E.; Griffin, P. R.; Wertz, I. E.; Lander, G. C. Molecular Glue CELMoD Compounds Are Regulators of Cereblon Conformation. *Science* **2022**, *378* (6619), 549–553.

(32) Li, T.; Robert, E. I.; van Breugel, P. C.; Strubin, M.; Zheng, N. A Promiscuous Alpha-Helical Motif Anchors Viral Hijackers and Substrate Receptors to the CUL4-DDB1 Ubiquitin Ligase Machinery. *Nat Struct Mol Biol* **2010**, *17* (1), 105–111.

(33) Li, T.; Chen, X.; Garbutt, K. C.; Zhou, P.; Zheng, N. Structure of DDB1 in Complex with a Paramyxovirus V Protein: Viral Hijack of a Propeller Cluster in Ubiquitin Ligase. *Cell* **2006**, *124* (1), 105–117.

(34) Salladini, E.; Delauzun, V.; Longhi, S. The Henipavirus V Protein Is a Prevalently Unfolded Protein with a Zinc-Finger Domain Involved in Binding to DDB1. *Mol. BioSyst.* **2017**, *13* (11), 2254–2267.

(35) Kostelic, M. M.; Zak, C. K.; Liu, Y.; Chen, V. S.; Wu, Z.; Sivinski, J.; Chapman, E.; Marty, M. T. UniDecCD: Deconvolution of Charge Detection-Mass Spectrometry Data. *Anal. Chem.* **2021**, *93* (44), 14722–14729.

(36) Quetschlich, D.; Esser, T. K.; Newport, T. D.; Fiorentino, F.; Shutin, D.; Chen, S.; Davis, R.; Lovera, S.; Liko, I.; Stansfeld, P. J.; Robinson, C. V. NaViA: A Program for the Visual Analysis of Complex Mass Spectra. *Bioinformatics* **2021**, *37* (24), 4876–4878.